Pediatr Radiol (2017) 47:507–521
DOI 10.1007/s00247-017-3806-0

Gadolinium-based contrast agents in pediatric magnetic resonance imaging

Eric M. Gale[1] · Peter Caravan[1] · Anil G. Rao[2] · Robert J. McDonald[3] · Matthew Winfeld[4] · Robert J. Fleck[5] · Michael S. Gee[6]

Received: 20 September 2016 / Revised: 16 November 2016 / Accepted: 10 February 2017 / Published online: 12 April 2017

Abstract Gadolinium-based contrast agents can increase the accuracy and expediency of an MRI examination. However the benefits of a contrast-enhanced scan must be carefully weighed against the well-documented risks associated with administration of exogenous contrast media. The purpose of this review is to discuss commercially available gadolinium-based contrast agents (GBCAs) in the context of pediatric radiology. We discuss the chemistry, regulatory status, safety and clinical applications, with particular emphasis on imaging of the blood vessels, heart, hepatobiliary tree and central nervous system. We also discuss non-GBCA MRI contrast agents that are less frequently used or not commercially available.

Keywords Children · Contrast agent · Gadolinium-based contrast agent · Magnetic resonance imaging · Safety

✉ Michael S. Gee
msgee@partners.org

[1] Department of Radiology,
The Martinos Center for Biomedical Imaging,
Massachusetts General Hospital, Harvard Medical School,
Boston, MA, USA

[2] Department of Radiology and Radiological Science,
Medical University of South Carolina, Charleston, SC, USA

[3] Department of Radiology, College of Medicine,
Mayo Clinic, Rochester, MN, USA

[4] University of Pennsylvania Perelman School of Medicine,
Philadelphia, PA, USA

[5] Department of Pediatric Radiology,
Cincinnati Children's Hospital Medical Center,
Cincinnati, OH, USA

[6] Division of Pediatric Imaging, Department of Radiology,
MassGeneral Hospital for Children, Harvard Medical School,
55 Fruit St., Ellison 237, Boston, MA 02114, USA

Introduction

Magnetic resonance imaging (MRI) offers high-resolution assessment of tissue anatomy and cellular composition without the need for ionizing radiation and is thus ideally suited for evaluation of pathological processes throughout the body, especially in the pediatric population [1–3]. The value of an MRI examination can be further increased by administration of a gadolinium-based contrast agent (GBCA) to characterize visceral organ lesions, stage malignancies, assess infectious and inflammatory processes, and evaluate vascular abnormalities [1, 4]. The advantages conferred by GBCAs can be particularly attractive in the context of pediatric patients because of the desire to avoid invasive diagnostic procedures in this population and the often smaller size of detected lesions compared with adults.

In this review article we summarize the chemistry related to the clinical use and safety of GBCAs, the regulatory status of the commercially available GBCAs, well-documented and newly raised safety concerns associated with GBCAs, and the clinical applications of GBCAs in imaging the vasculature, heart, hepatobiliary tree and central nervous system in children. We also provide a short discussion of clinically available non-GBCA contrast media, including the pediatric imaging with commercially available ultra-small iron oxide nanoparticles and newly emergent contrast agents that are not yet in clinical use.

Gadolinium-based contrast agents

Biophysics and chemistry relevant to the clinical use of GBCAs

MRI contrast reflects subtle differences in the endogenous magnetic properties of different tissues [2, 3]. In MRI, typically the hydrogen atoms of water and mobile lipids are

detected, and water and fat can be distinguished by their different chemical shifts (different frequencies for detection). Contrast can arise from differences in water content among tissues, i.e. proton density. Contrast can also be created by exploiting the different properties of water in local environments, e.g., distinguishing flowing water (blood) from stationary water (tissue), or by making images weighted to the rate of water diffusion. In a magnetic field, water molecules are characterized by their relaxation times: T1, T2, T2* and T1ρ. Differences in the local magnetic environment of the tissue cause variance in these relaxation times, and scans can be designed or weighted to reflect the tissue-dependent differences in relaxation rates. Relaxation times can also be affected by the presence of an exogenously administered contrast agent [5]. Most contrast-enhanced examinations take advantage of the potent T1-relaxation properties of GBCAs, which generate positive contrast in T1-weighted scans [4].

No other element is as well-suited to generate positive image contrast as gadolinium [4, 6, 7]. In its free, unchelated state, the gadolinium ion is toxic at the doses required for MRI; it is also insoluble. GBCAs must be formulated in a way that results in high water solubility and also shields the child from exposure to the free gadolinium ion. All GBCAs thus comprise gadolinium housed within an organic molecule, termed a chelate from the Latin for "claw," that envelops the gadolinium ion in order to block interactions between gadolinium and proteins or cells [6–8]. The chelate component in all clinically used GBCAs is designed to bond to eight positions on the gadolinium ion, thus maintaining a tight hold to sequester the toxic metal ion. The generic names and molecular structures of the nine GBCAs approved by the U.S. Food & Drug Administration (FDA) are depicted in Fig. 1 (trade names in parentheses).

The contrast generating efficacy of GBCAs is measured by a property termed relaxivity [6, 7]. Relaxivity describes the capability of a contrast agent to shorten water proton relaxation rates (1/T1, 1/T2), normalized to the contrast agent concentration, Eq. 1. Relaxivity is denoted r_1 or r_2 when referring to T1 or T2 shortening, respectively, and has units of $(mmol/L)^{-1}*s^{-1}$.

$$r_i = \Delta(1/T_i)/[\text{GBCA}] \text{ where i} \quad (1)$$
$$= 1, 2 \text{ and } [\text{GBCA}] \text{ is the GBCA concentration}$$

GBCA relaxivity is dictated by the molecular structure and by the dynamic solution behavior of the gadolinium-containing molecule [4, 6, 7, 9–12]. A direct bonding interaction between gadolinium and at least one water molecule is a requisite to achieving high relaxivity. However the water must only be bound to gadolinium transiently and be in rapid

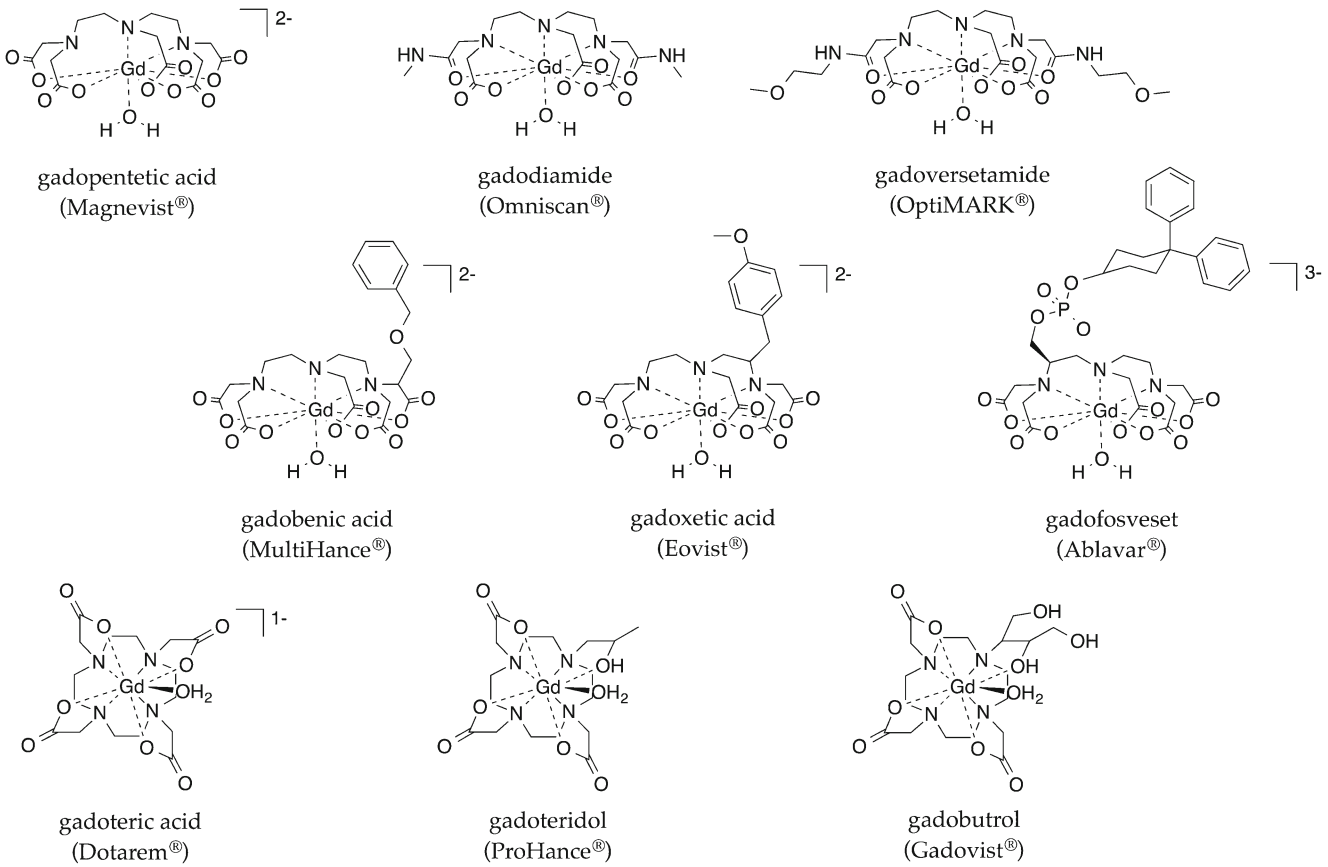

Fig. 1 Molecular structure and formal charge of the gadolinium-containing component of the nine gadolinium-based contrast agents approved by the U.S. Food & Drug Administration, with proprietary names in parentheses

exchange in order efficiently transfer the magnetic relaxation effect of gadolinium throughout the bulk water. Relaxivity also reflects the rate at which the GBCA rotates in solution. In most cases slower rotation translates to higher relaxivity; the magnitude of this effect is much greater at field strength ≤3 tesla (T). Slower rotation occurs when the GBCA is larger or if the molecule is transiently bound to protein, e.g., serum albumin. Each GBCA depicted in Fig. 1 possesses a single gadolinium-bound water molecule that exchanges with bulk water with a rate of 10^6 to 10^8 s^{-1} at 37°C, which is ideal for achieving high relaxivity. The GBCAs are of similar molecular weight and expected to rotate at a rate of ~10^{10} s^{-1} at 37°C. The r_1 values of each clinical GBCA in human whole blood at 37°C at various magnetic field strengths are summarized in Table 1 [13–19]. Given the similarities in structure and solution dynamics between these GBCAs, it is not surprising that there is generally little variation in relaxivity. The notable exceptions are gadofosveset, gadoxetic acid and gadobenic acid, which bind transiently and non-covalently to serum proteins. In blood, a fraction of these GBCAs exists in protein-bound, slowly rotating and high relaxivity form.

Resistance to gadolinium release from the GBCA chelate is dictated by two important physical properties, thermodynamic stability and kinetic inertness [6–8]. Thermodynamic stability is a measure of the chelate affinity for gadolinium under equilibrium conditions; kinetic inertness describes the rate of gadolinium release from the GBCA under dissociation driving conditions. The thermodynamic stability and kinetic inertness of different GBCAs are summarized in Table 1. It should be noted that experimental conditions used to generate

Table 1 Relaxivity (as $mM^{-1}s^{-1}$) in human whole blood, thermodynamic stability constant (logK) at pH 7.4, and dissocation half life ($t_{1/2}$) following zinc chloride challenge (2.5 mM GBCA, 2.5 mM zinc chloride, pH 7.0, 50 mM phosphate) or dissolution in pH 1 solution

GBCA	Relaxivity (1.5 T, 37°C)[j]	Relaxivity (3 T, 37°C)[j]	Relaxivity (7 T, 37°C)[j]	logK pH 7.4[k]	$t_{1/2}$ Zn challenge[l]	$t_{1/2}$ pH 1[l]
Gadopentetic acid (Magnevist)[a]	4.3±0.3	3.8±0.2	3.1±0.4	18.1	4.5 h	10 min
Gadodiamide (Omniscan)[b]	4.5±0.1	3.9±0.2	3.7±0.2	14.9	0.8 h	35 s
Gadoversatamide (OptiMARK)[c]	4.4±0.2	4.2±0.1	4.3±0.2	15.0	N/A	N/A
Gadobenic acid (MultiHance)[d]	6.2±0.4	5.4±0.3	4.7±0.1	18.4	N/A	N/A
Gadoxetic acid (Eovist/Primovist)[e]	7.2±0.2	5.5±0.3	4.9±0.1	N/A	25.0 h	N/A
Gadofosveset (Ablavar)[f]	27.7[m]	9.9[n]	5.4[o]	N/A	63.3 h	N/A
Gadoteric acid (Dotarem)[g]	3.9±0.1	3.5±0.3	2.8±0.4	18.8	>83 h	>1 month
Gadoteridol (ProHance)[h]	4.4±0.5	3.5±0.5	3.4±0.1	17.2	>83 h	2 h
Gadobutrol (Gadavist/Gadovist)[i]	4.6±0.2	4.5±0.2	4.2±0.2	N/A	N/A	24 h

h hours, *min* minutes, *s* seconds, *T* tesla

[a] Bayer HealthCare, Wayne, NJ

[b] GE Healthcare, Princeton, NJ

[c] Mallinckrodt, St. Louis, MO

[d] Bracco Diagnostics, Monroe, NJ

[e] Bayer HealthCare, Whippany, NJ

[f] Lantheus Medical Imaging, North Billerica, MA

[g] Guerbet, Bloomington, IN

[h] Bracco Diagnostics, Monroe, NJ

[i] Bayer HealthCare, Wayne, NJ

[j] Taken from [13]

[k] Taken from [14]

[l] Taken from [15, 16]

[m] Value in blood plasma taken from [17]

[n] Value in blood plasma taken from [18]

[o] Value in blood plasma taken from [19]

comparative metrics of kinetic inertness are non-physiological conditions that far exceed the challenge encountered in vivo [15, 16]. In other words, the inertness assays serve only to draw attention to the relative differences between GBCAs' resistances to degradation, and do not reflect actual rates of gadolinium release in vivo. However the extent of gadolinium deposition in tissue appears to be predicted by the relative kinetic inertness of the GBCAs [20, 21].

The thermodynamic and kinetic properties of each GBCA are a direct function of their unique chelate component. The molecular structures of chelates found in all clinically used GBCAs are classified based on the chelator type, either open-chain (sometimes referred to as linear) or macrocyclic, and the overall charge of the GBCA, either neutral or anionic (negatively charged, also referred to as ionic). Four classes exist: (1) open-chain neutral, which includes gadodiamide (GE Healthcare, Princeton, NJ) and gadoversetamide (Mallinckrodt, St. Louis, MO); (2) open-chain anionic, which includes gadopentetic acid (Bayer HealthCare, Whippany, NJ), gadobenic acid (Bracco Diagnostics, Monroe Township, NJ), gadoxetic acid (Bayer HealthCare) and gadofosveset (Lantheus Medical Imaging, North Billerica, MA); (3) macrocyclic neutral, which includes gadoteridol (Bracco Diagnostics) and gadobutrol (Bayer HealthCare); and (4) macrocyclic anionic, which includes gadoteric acid (Guerbet, Bloomington, IN) [6, 17]. Table 1 shows that the thermodynamic stability constants and rates of gadolinium release vary by orders of magnitude among GBCAs. The table also shows that kinetic inertness within the series of FDA-approved GBCAs can be organized in the following order: open-chain neutral < open-chain anionic <<< macrocyclic neutral < macrocyclic anionic.

Regulatory status

Table 2 summarizes the indicated use, recommended dose, incidence of adverse drug reactions (ADRs), and most

Table 2 Indicated use, regulatory approval status, recommended dose, adverse drug reaction (ADR) incidence, and frequently experienced ADRs for gadolinium-based contrast agents (GBCAs) approved by the U.S. Food & Drug Administration (FDA)

GBCA	FDA indicated use[a]	Approved for patients ages:	Recommended dose	ADR incidence	Most frequent ADR
Gadopentetate (Magnevist)	Visualization of lesions in the CNS, head, neck, and body[b]	≥2 years	0.1 mmol/kg	<4.8%	Headache, nausea, injection site reaction, dizziness
Gadodiamide (Omniscan)	Visualization of lesions in the CNS, intrathoracic[b], intra-abdominal, pelvic, and retroperitoneal regions	≥2 years	0.1 mmol/kg (0.05 mmol/kg for kidney)	<3.0%	Nausea, headache, dizziness
Gadoversatamide (OptiMARK)	Visualization of lesions in the CNS and liver	≥18 years	0.1 mmol/kg	35%	Injection site reaction, headache, vasodilation, taste perversion, dizziness, nausea, paresthesia, body pains, diarrhea, asthenia, rhinitis, dyspepsia
Gadobenic acid (MultiHance)	Visualization of lesions in the CNS, MR angiography of the renal and aorto-ilio-femoral vessels	≥2 years	0.1 mmol/kg	10.4% (>18 years old) 6.5% (2–17 years old)	Nausea, vomiting, feeling hot, injection site reaction, headache, pyrexia, hyperhidrosis, dysgeusia, paresthesia, dizziness
Gadoxetic acid (Eovist/Primovist)	Detection and characterization of lesions in the liver	≥18 years	0.025 mmol/kg	4.0%	Nausea, headache, feeling hot, dizziness, back pain, vomiting, blood pressure rise, injection site reactions
Gadofosveset (Ablavar)	MR angiographic evaluations of aortoiliac occlusive disease	≥18 years	0.03 mmol/kg	<1.0%	Pruritus, headache, nausea, vasodilation, paresthesia
Gadoteric acid (Dotarem)	Visualization of lesions in the CNS	≥2 years	0.1 mmol/kg	3.9% (>18 years old) 4.3% (2–17 years old)	Nausea, headache, injection site pain or coldness, burning sensation
Gadoteridol (ProHance)	Visualization of lesions in the CNS, head and neck	≥2 years	0.1 mmol/kg	1.4%	Nausea, taste perversion
Gadobutrol (Gadavist/Gadovist)	Visualization of lesions in the CNS	All ages	0.1 mmol/kg	4.0%	Headache, nausea, injection site reactions, dysgeusia, feeling hot

CNS central nervous system

[a] All information is taken from the FDA package inserts

[b] Excluding the heart

frequent ADRs for the nine FDA-approved GBCAs. ADRs are rare and the most frequently encountered adverse effects are not life-threatening. However the FDA boxed warnings state that acute kidney injury and cardiac arrest have been observed following administration of GBCAs to patients with severe renal impairment.

Most GBCAs are approved for use in patients ages 2 years and older, excepting gadoversetamide, gadoxetic acid and gadofosveset, which are approved only for patients 18 years and older. As a result, the use of GBCA in many pediatric patients is an off-label indication. Gadobutrol is the only GBCA that has received FDA approval for use in children younger than 2 years, although gadoteric acid is actively being evaluated in children younger than 2 [22]. American College of Radiology (ACR) guidelines for GBCA usage in children generally reflect those outlined for adults [23]. However it is worth noting that few published studies have concentrated on adverse drug reactions of GBCAs in children.

Safety

In 2006, a direct link was established between GBCAs and the onset of nephrogenic systemic fibrosis (NSF), a rare but potentially fatal fibrotic dermopathy, in renal-impaired patients [24, 25]. The FDA responded in 2007 by labeling all GBCAs with a boxed warning that advises against exceeding the recommended dose and against frequent repeat GBCA-enhanced examinations in patients with compromised renal function [26, 27]. Three GBCAs (gadodiamide, gadoversetamide, gadopentetic acid) are currently FDA-contraindicated in patients with glomerular filtration rate (GFR) <30 mL/min/1.73 m^2. The ACR recommends screening GFR of any patients with known or suspected renal impairment and advises against the use of any GBCA in patients with GFR <30 mL/min/1.73 m^2, suffering acute kidney injury, or requiring dialysis [23].

NSF risk is believed to increase with diminishing renal function. GBCAs are cleared primarily through renal filtration and the GBCA dwell time is significantly prolonged in cases of renal impairment. For example, it was shown that the clearance half-life of gadobenic acid extends from 2 h in patients with normal renal function, whereas in patients with GFR of 31–60 mL/min/1.73 m^2 it extends to 6.1±3.0 h, and in patients with GFR of ≤30 mL/min/1.73 m^2 it extends to 9.5±3.1 h [28]. Clearance half-lives of more than 30 h have been observed in cases of severe renal impairment [29]. Other GBCAs exhibit a comparable GFR dependence on clearance half-life [30, 31].

The mechanistic underpinnings of NSF are unknown, although a correlation between NSF incidence and GBCA kinetic inertness supports exposure to de-chelated gadolinium as a nidus of the disease. A data-mining analysis discussed in a 2015 FDA briefing showed that the proportional reporting ratio (PRR) and relative reporting ratio (RRR) of NSF cases associated with exposure to different GBCAs correlate inversely with kinetic inertness [29]. The European Medicines Agency classification of GBCAs as posing high, intermediate or low risk for NSF is a direct reflection of GBCA inertness, with the more rapidly dissociating GBCAs (gadodiamide, gadoversetamide, gadopentetic acid) classified as high risk [32].

There are few reported cases of NSF in pediatric patients [33]. GBCAs exhibit similar clearance profile across all ages, and body weight is the primary determinant of clearance half-life in patients 2 years and older [34]. Renal function is still maturing up to 2 years of age and infants could be at greater risk for GBCA-associated toxicity. Quantification of gadobutrol clearance in 43 children with normal renal function ages <1 month to 2 years revealed that clearance rates are slightly decelerated with decreasing age [35]. We are unaware of any formal studies correlating NSF risk to renal function or individual GBCAs in children. However it is recommended that the same precautions applied to adults with known or suspected renal insufficiency be applied to children.

A number of recent reports point toward non-negligible gadolinium (Gd) accumulation in the brains of patients with normal renal function who have received multiple GBCA injections. Suspicions were raised following a 2013 report of hyperintense dentate nuclei and globus pallidus in contrast-free T1-weighted scans of patients having previously received multiple GBCA-enhanced examinations [36]. A subsequent study demonstrated that the dentate nucleus-to-pons and globus pallidus-to-thalamus signal-intensity ratios in contrast-free scans were highly correlated to the number of prior GBCA injections received [37]. A 2015 study on autopsy specimens confirmed Gd accumulation in the central nervous system (CNS) as the source of brain-tissue hyperintensity [38]. The risk of CNS gadolinium accumulation also appears to correlate with GBCA class and is likely related to the level of kinetic inertness. Recent studies have demonstrated that the dentate nucleus-to-cerebellum signal-intensity ratio was strongly correlated to the number of prior contrast-enhanced MR examinations for patients having exclusively received injections of a linear GBCA but not for patients who only received a macrocyclic GBCAs [39, 40], suggesting that macrocyclic contrast agents deposit gadolinium in tissues at a lower level than linear agents. In 2015, a retrospective analysis of unenhanced brain scans recorded on a single pediatric patient receiving multiple injections of gadopentetic acid between the ages of 5 and 21 revealed dose-dependent hyperintensity patterns consistent with those observed in adults [41].

There is emerging evidence of potential GBCA deposition from MRI studies outside the brain, including a 2016 autopsy study demonstrating elevated bone levels of gadolinium by mass spectrometry in adults with normal renal function who had prior contrast MRI with either a linear or macrocyclic GBCA [42]; additionally, another study demonstrated a positive correlation between liver gadolinium and iron concentrations in pediatric patients with iron overload undergoing MRI with the

macrocyclic agent gadoteric acid [43]. Interestingly, this last study also showed a decrease in gadolinium liver concentration in patients undergoing iron chelation therapy, suggesting a potential treatment strategy for gadolinium tissue deposition.

The health risks posed by tissue deposition of gadolinium not associated with NSF remain unclear, as do the mechanisms driving gadolinium accumulation. In 2015 the FDA announced plans for an investigation to identify and evaluate the safety risks associated with this phenomenon. Future investigation is also needed to quantify and determine the risks associated with gadolinium accumulation in the pediatric population.

Review of pediatric clinical applications of GBCAs

Gadolinium-based contrast agents are useful and increase diagnostic efficacy in many situations, although the incremental benefit of GBCA use might vary widely depending on the body part imaged, patient size and intravenous access, and the clinical indication. Specific clinical applications of GBCA in pediatric MRI are discussed next.

Magnetic resonance angiography and venography

The clinical indications for body MR angiography and MR venography in pediatric imaging are numerous, with new applications continuously developing. Among their more common uses are in the evaluation of vascular tumors and malformations, vasculitis, aortic coarctation, renal artery stenosis, portal hypertension and thoracic outlet syndrome. These modalities can also be used in preoperative planning, such as prior to liver transplantation or for living-donor evaluation [44, 45].

Both non-contrast and contrast-enhanced techniques can be used to perform MR angiography and MR venography. Non-contrast sequences are attractive for use in the pediatric population for several reasons, including eliminating the potentially deleterious effects of contrast agents and allowing for repeat sequences in case of excessive artifact [46]. Nevertheless, contrast-enhanced techniques have numerous advantages, which include fast acquisition with high spatial and contrast resolution and the potential to perform dynamic time-resolved imaging [47]. Therefore the choice of how to perform body MR angiography and MR venography should be based on the clinical question and patient-specific factors, such as renal function and the ability to breath-hold.

Contrast-enhanced MR angiography can be performed with routine extracellular gadolinium-based agents. Because signal-to-noise ratio is a key parameter in producing quality body MR angiographic images, agents with higher T1 relaxivity, which produce greater intravascular signal [44], are preferred if available. Nonetheless an optimally performed study with any gadolinium-based contrast agent should produce diagnostic images. Intravenous contrast agent is dosed based on weight, a conversion that is specific to the agent chosen. At some institutions, contrast agent is diluted in saline up to 1:6 as a means of lengthening bolus time to avoid missing peak enhancement and to minimize contrast volume-related artifacts, particularly in small children, who require as little as 1–2 mL of contrast agent based on weight. Administration of contrast agent is typically done using a power injector, with rates ranging 2–3 mL/s for MR angiography and approximately 1 mL/s for MR venography; hand-injected boluses can typically only be done at a rate of 1.5–2 mL/s and may be uneven. A saline chaser of 10–20 mL might also be used to help achieve smooth enhancement peak for optimal imaging, though volume overload could be a concern in very small children [45].

The success of MR angiography and MR venography techniques lies in the timing of the bolus. Two strategies can be employed to optimize timing: test bolus and automated triggering. With a test bolus, a small volume of contrast agent is administered and the desired region of interest is continuously scanned until a target signal intensity is achieved, thereby determining the appropriate scan delay after injection of the full contrast dose. With automated triggering, a similar continuous monitoring strategy is used after injection of the full bolus, with scanning beginning when a target signal intensity is reached at the region of interest [44].

The workhorse sequence in contrast-enhanced MR angiography and MR venography is a T1-weighted spoiled gradient echo with minimal repetition time (TR) and echo time (TE) and low flip angles [44, 48]. These sequences provide high spatial resolution but are sensitive to motion artifact and typically take 15–30 s to acquire [48], which can limit their use in children who are unable to sufficiently breath-hold. Furthermore, multi-phase acquisitions are limited by the time to acquire the sequence and the ability of the child to perform multiple breath-holds in a relatively short period of time. Time-resolved techniques are also available, such as keyhole imaging, in which only the center of k-space is sampled repeatedly with high temporal resolution while a contrast bolus progresses through the region of interest, with complete k-space acquisition occurring either at the beginning or the end of imaging. The center of k-space provides contrast data while the periphery supplies fine detail, leading to a rapid high-resolution scan. An additional phase can be acquired before contrast agent arrival for subtraction, resulting in improved signal-to-noise ratio [49]. Many institutions use this technique with 2.5-s temporal resolution. Bolus timing is not a concern with this technique.

One agent with specific properties that aid in effective MR angiography and MR venography imaging is gadofosveset. Gadofosveset is distinct in that it binds intravascular albumin and circulates throughout the blood pool for an extended period of time [50]. Optimal timing of a contrast bolus is still

required to obtain true first-pass arterial phase imaging; however, steady-state vascular imaging can be performed up to 1 h or longer after injection [44]. This gives ample opportunity to obtain images in children who have difficulty lying still, and also allows for multiple stations to be imaged without sacrificing image quality (Fig. 2). Many institutions use gadofosveset routinely for all contrast-enhanced MR angiography and MR venography studies. Of note, at the time of publication of this manuscript, gadofosveset was no longer available for distribution in the United States and alternative MRI contrast agents such as ferumoxytol were being explored for cardiovascular MR indications.

Cardiac magnetic resonance imaging

Cardiac applications of GBCA include five general categories: angiography, late gadolinium enhancement (LGE), early enhancement, myocardial perfusion, and pre- and post-T1 mapping. MR angiography, myocardial perfusion and LGE are the most widely used applications of GBCA technique when performing cardiovascular MR in children, particularly in the setting of congenital heart disease.

Performing pediatric cardiovascular MRI presents several challenges: (1) small volumes of injected contrast agent result in very transient first-pass luminal opacification; (2) many children are unable to hold their breath when imaged awake; (3) often sedation is chosen over intubation with general anesthesia for safety reasons, and (4) small size and variable and high heart rates lead to fast circulation times, requiring more precision and planning for the timing of imaging after contrast administration. Fortunately, both hardware and imaging techniques have evolved over the years, making cardiovascular MRI with GBCA in children relatively routine. For nearly all purposes in pediatric cardiovascular imaging, some form of accelerated time-resolved imaging (Fig. 3) is used [47, 51]. Each acquisition is dynamic and the length of time for each acquisition is tailored for the clinical question and depends on individual patient characteristics. If one does not need to

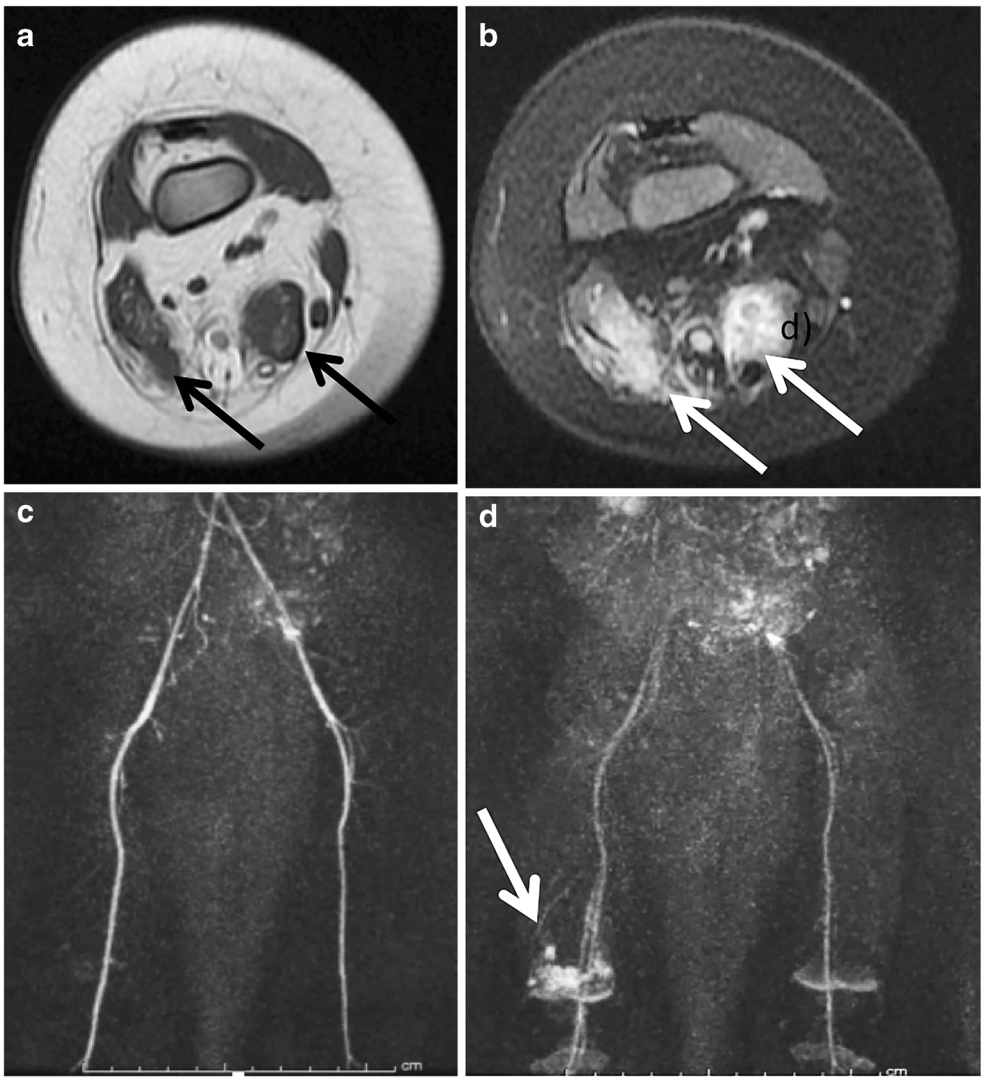

Fig. 2 Gadofosveset MR angiography in a 3-year-old boy with acquired knee contracture. **a**, **b** Axial T1-weighted (**a**) and T2-weighted fat-suppressed (**b**) MR images through the distal thigh demonstrate abnormal signal in the biceps femoris and semimembranosus muscles (*arrows*), with infiltration of the intervening fat. **c**, **d** MR angiography images after administration of gadofosveset during arterial (**c**) and venous (**d**) phases demonstrate venous-predominant (**d**; *arrow*) enhancement of the same region. Pathological diagnosis was fibroadipose vascular anomaly. Images courtesy of Hansel Otero, MD, Children's National Hospital, Washington, DC

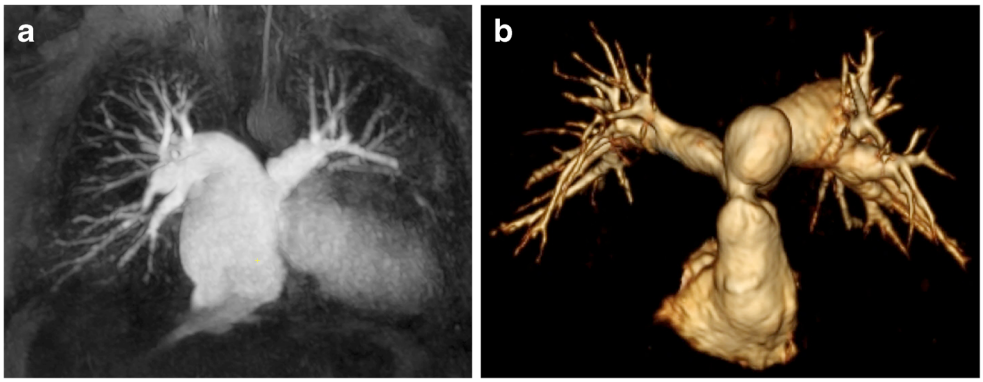

Fig. 3 Cardiac MR angiography performed with GBCA depicts congenital heart disease and surgical anatomy. **a** Coronal maximum-intensity projection obtained from a time-resolved angiogram in a 15-year-old boy shows the post-surgical appearance of a classic Fontan operation. **b** Coronal 3-D surface-rendered display of the pulmonary outflow tract and arteries from a 40-year-old man with ventricular septal defect and aortic coarctation treated with pulmonary artery banding shows narrowing at the main pulmonary artery with post-stenotic aneurysmal dilation. *GBCA* gadolinium-based contrast agent

separate the pulmonary phase from the systemic circulation and venous phase, temporal resolution of each dynamic can be relatively long, and longer acquisition time can be used to increase spatial resolution. If the converse is needed, fast dynamic imaging can be achieved by reducing spatial resolution. The image acquisition is accelerated by taking advantage of spatial redundancy using surface coil arrays and redundancy of information in k-space over time, resulting in high temporal and spatial resolution [51].

The concepts of MR angiography were discussed in detail in the previous section. However some techniques are relevant to the pattern of circulation in congenital heart disease and repaired congenital heart disease, and these are worthy of mention. The circulation of contrast agent from a venous injection in a child who has undergone a total cavopulmonary connection (Fontan) is dependent on whether an upper or lower limb is injected for first-pass angiography because of flow splits between inferior vena cava and superior vena cava flow [52]. In the past these children were often injected simultaneously or via a split bolus injection into both an upper and lower extremities for viewing the blood flow trajectory associated with each injection. However it is now more common to use a blood-pool agent, such as gadofosveset or ultra-small superparamagnetic iron oxide, to image during equilibrium [53], and some centers are advantageously using the blood-pool contrast agent to optimize 4-D flow acquisition [54, 55].

The next most frequently used application of GBCA in imaging heart disease in children is late gadolinium enhancement. This technique was initially demonstrated on CT using iodinated contrast agents [56], but it has really increased in clinical application with MRI and GBCAs [57]. The technique is based on the GBCA's initial entry into and subsequent washout from normal myocardium at defined time intervals, with abnormal myocardium demonstrating GBCA retention for an extended period of time (Fig. 4). This phenomenon can be exploited by delayed imaging with a T1-weighted pulse sequence after the typical time interval of GBCA washout from normal myocardium to visualize LGE. The contrast between normal and abnormal myocardium is increased by choosing an inversion time that suppresses the signal intensity of the normal myocardium [58]. Abnormal myocardium can be thought of as having increased extracellular space [58] and collagen deposition as a result of myocardial cell death.

Generally LGE cannot be visualized until there is a geographically large enough area to enhance several adjacent voxels such as after ischemia secondary to a myocardial infarction in adults; however imaging myocardial infarction in the pediatric and congenital patient population is uncommon. Occasionally imaging is performed specifically looking for infarction in children and can be seen when coronary arteries are injured during surgical repair of congenital heart disease or in Kawasaki disease. More commonly LGE is applied in children with cardiomyopathies, including hypertrophic cardiomyopathy, Duchenne and Becker muscular dystrophies, and deposition diseases where its presence has predictive implications [59, 60].

A promising development under the umbrella of LGE is the use of T1-mapping pre- and post-gadolinium to calculate extracellular volume fractions [61]. This technique allows fractionation of the myocardium into cellular and interstitial components and can be advantageous in diseases such as cardiomyopathies, myocardial inflammation and deposition disorders before they exhibit a geographic area of LGE following coalescence of fibrosis or extracellular protein deposition. The ability to visualize and quantify extracellular fibrosis prior to the appearance of LGE is proving to be a powerful imaging technique. Additionally, first-pass perfusion [62] is an infrequent technique in children that is most commonly used to assess for myocardial ischemia in conditions such as Kawasaki disease, vasculitis, elevated serum troponin levels, evaluation after arterial switch operations, or in evaluation of cardiac masses [63, 64].

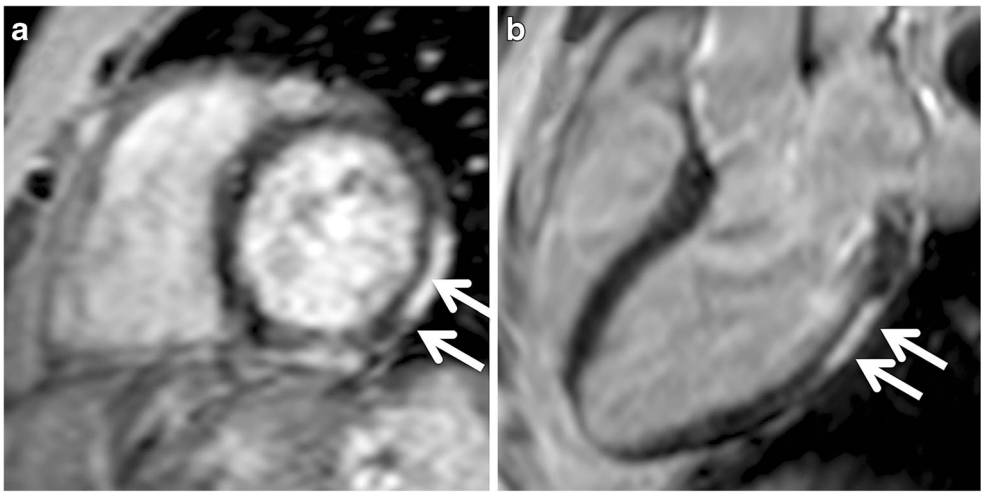

Fig. 4 Cardiac MRI with late gadolinium enhancement in a 9-year-old boy with Duchenne muscular dystrophy, initial evaluation of cardiomyopathy. **a** Short-axis slice through the base of the heart shows sub-epicardial enhancement in the basal anterolateral/mid-anterolateral segments of the left ventricle (*arrows*). **b** Orthogonal slice in the three-chamber plane confirms the presence of the late gadolinium enhancement (*arrows*)

One final use of GBCA in pediatric cardiac imaging is for assessment of myocarditis. Tissue characterization to aid in the diagnosis of myocarditis is the main contribution of cardiac MRI. MR pulse sequences used to characterize myocardial abnormalities in the setting of myocarditis include T2-weighted imaging, first-pass perfusion, T1-weighted myocardial early gadolinium enhancement and LGE [65, 66]. Typically the areas of increased T1-weighted signal intensity are defined by increased signal relative to skeletal muscle, or in the case of myocarditis with myositis an absolute increase in myocardial signal intensity of greater than 45% is required [66]. Native T1 mapping, T2 mapping and T1 mapping during early and late washout of GBCA are promising quantitative techniques that will be forthcoming in the near future [67, 68].

Hepatobiliary magnetic resonance imaging

Extracellular GBCAs traditionally have been used for routine hepatobiliary imaging because of their utility in detecting focal lesions in solid visceral organs. However hepatocyte-specific MR contrast agents, because of their accumulation in hepatocytes and subsequent biliary excretion, are preferred for detection of focal hepatic lesions as well as characterization of hepatic lesions seen on prior imaging. Biliary anatomy can also be assessed because of the biliary excretion of these contrast agents [69]. In general, images following hepatocyte-specific GBCA administration are acquired after a longer time interval following injection compared with standard extracellular agents. Hepatocyte-specific contrast agents available for clinical use include gadoxetic acid, gadobenate meglumine and the manganese (Mn)-based agent mangafodipir (Teslascan; GE Healthcare). Mangafodipir is no longer in clinical use.

Gadoxetic acid has 50% hepatobiliary and 50% renal excretion. Following intravenous injection, gadoxetic acid distributes into the vascular and extravascular spaces during the arterial, portal venous and late dynamic phases. Gradually, there is hepatocyte uptake and subsequent excretion into the biliary tree. The hepatocyte uptake of gadoxetic acid occurs via the organic anion transporter polypeptides OATP1B1 and B3, located at the sinusoidal membrane and biliary excretion via the multidrug-resistance-associated proteins MRP2 [70]. Gadoxetic acid was FDA-approved 2008 as an intravenous contrast agent for evaluation of known or suspected focal liver disease in adults. Safety and efficacy of this drug in children have not been established. The recommended dose of administration is 0.1 mL/ kg body weight (0.025 mmol/ kg body weight) to be administered as an intravenous bolus injection at rate of 2 mL/s in adults. The standard delay for hepatobiliary phase imaging with gadoxetic acid is 20-min post-injection. Of note, significant hepatic dysfunction can lead to decreased hepatobiliary excretion of gadoxetate that can alter the contrast between normal liver parenchyma and focal lesions during hepatobiliary phase imaging. Anionic drugs that are mainly excreted into the bile such as rifampicin can also reduce the hepatic contrast enhancement and biliary excretion of the drug [71].

Gadobenic acid undergoes less hepatobiliary excretion (5%) relative to gadoxetic acid, with the rest undergoing renal excretion. The mechanism of hepatocyte uptake and excretion into the biliary system is similar to that of gadoxetic acid. This contrast agent was approved by the FDA in 2004 as an intravenous contrast agent for use in MRI of the central nervous system in adults and children older than 2 years to visualize lesions with abnormal blood–brain barrier or abnormal vascularity of the brain, spine and associated soft tissues. Hepatic dysfunction does not have significant impact on the pharmacokinetics of this drug; however the elimination half-life significantly increased in patients with moderate and severe renal dysfunction. The recommended dose for intravenous administration in adults is 0.2 mL/ kg body weight (0.1 mmol/ kg body weight) followed by a saline flush. The high relaxivity and longer intravascular circulation time of gadobenic acid compared with other extracellular GBCA is advantageous for evaluation of vascular structures.

Both gadoxetic acid and gadobenic acid are extensively used for problem-solving in hepatobiliary imaging. Indications for these agents include staging of primary hepatic malignancies and detection of hepatic metastases; focal hepatic lesion characterization, particularly in cases of suspected focal nodular hyperplasia; and assessment of anatomy, function, and integrity of the biliary tree. Focal nodular hyperplasia shows accumulated contrast agent on hepatobiliary phase imaging, while primary hepatic malignancies, hepatic metastases and hepatocellular adenomas demonstrate low signal intensity (Fig. 5). Hemangiomas also might demonstrate low signal intensity on hepatocyte-phase imaging but typically demonstrate nodular centripetal enhancement in the venous phase and contrast retention in the equilibrium phase (2–5 min post-injection). Longer delays (30–120 min post-injection) are often required to evaluate the biliary system using hepatobiliary GBCAs. Because of the increased biliary excretion of gadoxetic acid compared with gadobenic acid, the hepatocyte phase during gadoxetic acid imaging is much earlier (20 min post-injection) compared to gadobenic acid (60–120 min post-injection). As a result, gadoxetic acid has almost completely replaced gadobenic acid in North America for hepatobiliary evaluation in adults [71]. Gadoxetate and gadobenate have similar safety profiles, with rarely occurring serious ADRs. In two separate studies, no cases of NSF were reported during a 2-year follow-up of patients with impaired renal function who received either gadoxetate or gadobenate [72, 73]. Use of hepatobiliary GBCAs in children should be limited to cases in which they are likely to provide added diagnostic value after consideration of risks and benefits.

Central nervous system MRI

MRI plays a critical role in the evaluation of central nervous system pathology in children [1]. Specific diseases that are evaluated by MRI in children include stroke, solid intracranial masses, congenital central nervous system (CNS) and vascular malformations, hereditary metabolic diseases, hypoxic–ischemic injury, demyelinating disease, epilepsy, inflammatory diseases and infections. Standard indications for GBCAs in MR imaging of the pediatric CNS include suspected infection, characterization of focal masses, and assessment of activity of demyelinating or inflammatory diseases. For these indications, extracellular GBCAs are used with post-contrast images obtained at least 3–5 min after contrast injection, corresponding to the extravascular equilibrium phase of CNS enhancement [74].

For cases in which evaluation of vascularity/perfusion using MR angiography is desired, both extracellular and blood-pool GBCAs have been used in the pediatric population. Gadofosveset is the only blood-pool GBCA in the United States that is approved for clinical use in adults, but it has been successfully used as an off-label agent in numerous pediatric imaging studies [75, 76]. Injection of GBCA followed by high-temporal-resolution imaging in the arterial and venous

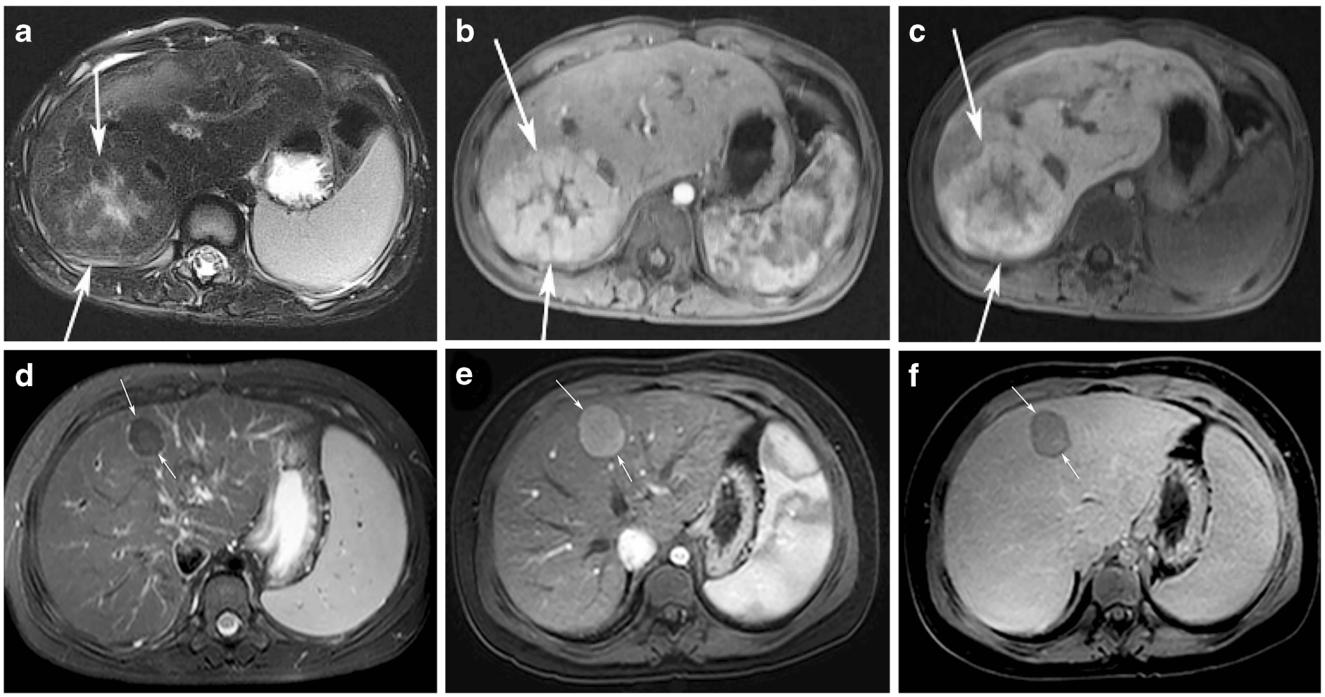

Fig. 5 Hepatobiliary MR imaging using gadoxetic acid. T2-weighted fat-suppressed (**a**, **d**) and arterial phase (**b**, **e**) and 20-min hepatobiliary phase post-contrast (**c**, **f**) images. **a**–**c** Focal nodular hyperplasia in an 8-year-old girl demonstrates a T2-weighted hyperintense central scar (**a**, *arrows*), avid arterial-phase enhancement (**b**) and hepatobiliary contrast excretion (**c**). **d**–**f** Hepatocellular adenoma in a 10-year-old boy demonstrates low T2-weighted signal intensity (**d**, *arrows*), early arterial enhancement (**e**) and minimal hepatobiliary contrast excretion (**f**). Adenoma images courtesy of Jonathan R. Dillman, MD, Cincinnati Children's Hospital Medical Center

phases is a standard part of the MR angiography technique. Gadofosveset, because of its relatively long blood-pool half-life, allows for additional high-resolution or triggered steady-state image acquisition to delineate vascular anatomy [77]. Dynamic contrast-enhanced (DCE) and dynamic susceptibility-weighted contrast-enhanced (DSC) perfusion MRI may also be used to evaluate brain parenchymal perfusion in children with suspected stroke or to characterize microvascularity and aggressiveness of intracranial mass lesions [78]. In these techniques, extracellular GBCA is power-injected and high-temporal-resolution T1-weighted (DCE) or T2*-weighted (DSC) images are acquired before, during and after contrast administration. Subsequently pharmacokinetic perfusion maps of GBCA tissue enhancement, including cerebral blood volume and permeability transfer coefficient, can be generated.

Alternative MRI contrast agents

Superparamagnetic iron-oxide nanoparticles

Sub-microscopic particles of colloidal iron oxide, termed superparamagnetic iron-oxide nanoparticles (SPIONs), are extremely potent MR contrast agents [79]. The particles themselves are insoluble and intravenous contrast formulations are composed of particles functionalized with solubilizing carbohydrate coatings. The relaxivity properties, distribution and pharmacokinetics of SPION formulations are mostly dictated by particle size, but the choice of iron-oxide coating can also influence distribution [80]. In all FDA-approved SPION formulations, the particles exceed 10 nm in diameter and are thus unable to extravasate from the blood vessels or be filtered through the kidneys. The particles are taken up by tissues that participate in the reticuloendothelial system: liver, spleen and lymph nodes [81, 82]. Particles exceeding 80 nm in diameter are more rapidly accumulated within the reticuloendothelial system but smaller particles can exhibit circulatory half-lives on the order of days [83, 84].

SPION relaxivity is also influenced by particle size. SPIONs are best known for their high magnetic susceptibility and strong influence over T2* (signal loss); that is, they provide negative contrast. For larger particles, e.g., exceeding 40 nm in diameter, the T1 relaxivity is very low and these particles cannot be used for T1-weighted imaging. For smaller particles, T1 relaxivity can be very high at 1.5 T but decreases rapidly with increasing field strength. These particles, sometimes called ultra-small particles of iron oxide, can generate both positive and negative image contrast with T1-weighted or T2*-weighted imaging schemes, respectively [79].

Because of the major differences between the distribution and pharmacokinetics of GBCAs and SPIONs, the two classes of contrast agents can be used interchangeably in only a limited number of applications. Small SPIONs such as ferumoxytol (Feraheme, AMAG Pharmaceuticals, Lexington, MA) can substitute for GBCAs in MR angiography examinations [85]. Ferumoxytol particles are sufficiently small to partially evade the reticuloendothelial system and maintain a blood half-life of 12–14 h and to provide strong positive vessel-to-tissue contrast. The long circulatory half-life of ferumoxytol is very attractive for pediatric MRI. Whereas GBCAs provide a fleeting window for MR angiography that can be easily missed in the case of an uncooperative child, the substantially elongated angiographic window provided by ferumoxytol allows several attempts at diagnostic imaging from a single injection. The elongated acquisition window also offers an opportunity to collect sufficient data to construct high-quality motion-averaged images from free-breathing examinations.

SPIONs can also be used as an alternative to GBCAs (i.e. gadoxetic acid) to characterize hepatic lesions. The FDA-approved but commercially discontinued ferumoxide is a formulation of SPIONS ranging 80–120 nm in diameter, for this purpose. A similar formulation, termed ferucarbotran (Resovist, Bayer HealthCare), was approved for the European market but has also been commercially discontinued. Accumulation of SPIONS in the Kupffer cells found throughout liver parenchyma renders normal liver dark, while tissue devoid of Kupffer cells, such as hepatoma lesions, are hyperintense relative to healthy liver [80].

SPIONs can also be imaged after long time delays (24 h) to exploit their reticuloendothelial cell accumulation for lymph node characterization. For example, comparison of signal change pre- and post-SPION administration can be used to differentiate malignant from normal lymph nodes in T2*-weighted scans [86, 87]. SPION affinity for the reticuloendothelial system induces a large signal drop in normal lymph nodes, whereas signal remains largely unchanged in malignant lymph nodes in which the macrophage population is reduced by the presence of tumor cells.

Ferumoxytol is the only SPION formulation currently marketed in the United States. Ferumoxytol received FDA approval as an intravenous iron supplement for anemic patients but has been administered for off-label use in MR angiography [85, 88]. There are very few accounts of ferumoxytol-enhanced MRI examinations in children. A 2015 retrospective analysis of ferumoxytol-enhanced abdominal MR angiography and cardiac MRI in patients ages 3 days to 18 years concluded that ferumoxytol administered at dosages of 1.5–3.0 mg iron (Fe) per kilogram body weight provides highly diagnostic angiographic images [89]. A 2016 evaluation of ferumoxytol in pediatric patients with severe chronic kidney disease demonstrated that diagnostic MR venography can be achieved using 4.0 mg Fe per kilogram body weight [90]. Conclusions drawn from the ferumoxytol-enhanced imaging were in accord with the conclusions drawn from any additional imaging or invasive procedures, without exception.

Another study evaluated ferumoxytol-enhanced dynamic susceptibility contrast in assessing the vascularization of brain tumors in children [91]. Relative cerebral blood flow and relative cerebral blood volume were quantified and the authors concluded that this vascular information was highly useful in guiding resection plans and postoperative monitoring.

Serious ADRs from ferumoxytol occur with higher incidence than with GBCAs and have led to the FDA to issue a boxed warning about potential serious allergic reactions [92]. Severe hypersensitivity reactions were observed in 0.2% of patients during clinical trials; 79 cases of severe anaphylaxis resulting from intravenous administration of ferumoxytol were reported to the FDA between 2009 and 2014, and 18 of these cases were fatal [92]. However a 2016 summary of ADR incidence in 68 patients ages ≤18 years who were experiencing tumors or undergoing kidney transplants reported 4 mild ADRs (2 experienced transient hypotension, 1 experienced nausea and 1 experienced an injection site reaction) [93]. Each of the pediatric ADRs was self-resolved. The authors acknowledge that a much larger pediatric patient cohort is required to assess the pediatric risk of severe ADRs observed in ferumoxytol-treated adults. Ferumoxytol is indicated for iron replacement therapy and is given as an intravenous dose of 510 mg to adults, which is approximately 7 mg/kg. Doses used for imaging are reported in the 1–4 mg/kg range.

Manganese-based contrast agents

Manganese induces magnetic relaxation via analogous mechanisms and with comparable potency to gadolinium [7, 94]. The manganese-based contrast agent mangafodipir (Teslascan) was FDA-approved for imaging of the hepatobiliary tree but was commercially discontinued [18, 94–98]. Mangafodipir is a manganese-chelate formulation that is partially dissociated in the bloodstream [99]. Dechelated manganese and a fraction of the intact mangafodipir are accumulated by hepatocytes and cleared via the hepatobiliary path, thus providing excellent hepatobiliary contrast. The chelate component of mangafodipir serves to attenuate manganese exposure, which is cardio-depressive when bolused at high concentrations [100, 101].

Manganese-based contrast agents (MBCAs) offer the most feasible possibility for an efficacious GBCA substitute and represent a highly attractive alternative in light of NSF and the recent discovery of gadolinium accumulation in the central nervous system. A small-molecule MBCA could reasonably substitute for a GBCA in any indication. Manganese is a biogenic element that is essential for human life, and the human body possesses mechanisms to process and tightly regulate manganese levels [102]. Thus the toxicity burden posed by dissociation of small amounts of manganese is very low compared to that of gadolinium. Mangafodipir, which is largely dissociated in vivo, was administered to thousands of patients with very low incidence of ADR and little apparent toxicity. The primary impediment to developing manganese-based substitute for GBCAs is the generally low thermodynamic stability and kinetic inertness of chelated manganese vs. chelated gadolinium. Manganese dissociating agents like mangafodipir provide more limited or specialized diagnostic information (e.g., imaging manganese-accumulating tissue such as liver) than intact and freely distributing contrast agents. However recent accounts of high-relaxivity, thermodynamically stable and kinetically inert manganese-chelate molecules support the possibility of MBCAs as potential GBCA alternatives [103].

Other MRI contrast agents

Not all MRI contrast agents generate contrast through magnetic relaxation. Contrast can also be generated by agents detected directly through non-water protons or heteroatoms (e.g., fluorine, carbon) [104–107], or indirectly via chemical exchange saturation transfer [19, 108]. Relaxation agents are generally detected with much greater sensitivity than agents detected by direct nuclear observation or chemical exchange saturation transfer and are truly the best candidates for multipurpose, freely distributing probes. To date, all FDA-approved MRI contrast agents are relaxation agents. However non-relaxation-inducing contrast agents have been meaningfully used in the clinical setting, particularly in the context of molecular imaging. Hyperpolarization can decrease the detection limit of directly detected nuclei by up to 6 orders of magnitude, reaching levels well below the detection limit of GBCAs. Direct detection of molecules labeled with hyperpolarized nuclei, such as 13C-polarized pyruvate, can be used to interrogate the metabolic profile of malignant tissue [109]. Hyperpolarized 129Xe and 3He have been utilized to characterize pulmonary gas uptake [110, 111]. Unfortunately hyperpolarized contrast agents are not shelf-stable because hyperpolarized states decay on the order of seconds to minutes. Thus imaging studies using hyperpolarized contrast agents require an on-site polarizer and near-perfectly timed data acquisition.

Conclusion

Administration of a GBCA can add tremendous value to pediatric MRI examinations. GBCAs provide positive contrast to enhance the conspicuity of lesions and enable dynamic imaging of the vasculature and tissue perfusion over time. Although adverse reactions to GBCAs occur with low incidence, GBCAs pose a risk of severe toxicity in patients with renal impairment and new evidence raises the possibility of gadolinium accumulation in the central nervous system of patients requiring multiple GBCA-enhanced scans. Radiologists should ensure that GBCA is likely to add diagnostic value to a pediatric

MRI study before administering contrast agent, especially in children likely to require multiple MRI exams over time. SPIONs such as ferumoxytol might be used in the place of GBCAs to image the blood pool and reticuloendothelial tissue, although they should be used with caution given their potential allergy risks.

Compliance with ethical standards

Conflicts of interest Dr. Gale has provided consulting services to Collagen Medical LLC, and has equity in Reveal Pharmaceuticals Inc. Dr. Caravan has research funding from Pfizer, Biogen and Agilent, has provided consulting services to Guerbet, and has equity in Collagen Medical LLC, Factor 1A LLC and Reveal Pharmaceuticals Inc. Drs. Rao, McDonald, Winfeld, Fleck and Gee have no potential conflicts of interest to disclose.

References

1. Bhargava R, Hahn G, Hirsch W et al (2013) Contrast-enhanced magnetic resonance imaging in pediatric patients: review and recommendations for current practice. Magn Reson Insights 6: 95–111
2. Young IR (2000) Methods in biomedical magnetic resonance imaging and spectroscopy. Wiley, Chichester
3. Edelman GM, Hesselink JR, Zlatkin MB et al (2006) Clinical magnetic resonance imaging — volume 3. Elsevier Health, St. Louis
4. Boros E, Gale EM, Caravan P (2015) MR imaging probes: design and applications. Dalton Trans 44:4804–4818
5. Carr DH, Bydder GM, Weinmann H-J et al (1984) Intravenous chelated gadolinium as a contrast agent in NMR imaging of cerebral tumors. Lancet 323:484–486
6. Caravan P, Ellison JJ, McMurry TJ et al (1999) Gadolinium(III) chelates as MRI contrast agents: structure, dynamics and applications. Chem Rev 99:2293–2352
7. Caravan P, Farrar CT, Frullano L et al (2009) Influence of molecular parameters and increasing magnetic field strength on relaxivity of gadolinium- and manganese-based T1-contrast agents. Contrast Media Mol Imaging 4:89–100
8. Gale EM, Atanasova I, Blasi F et al (2015) A manganese alternative to gadolinium for MRI contrast. J Am Chem Soc 137:15548–15557
9. Caravan P (2006) Strategies for increasing the sensitivity of gadolinium based MRI contrast agents. Chem Soc Rev 35:512–523
10. Caravan P (2009) Protein-targeted gadolinium-based magnetic resonance imaging (MRI) contrast agents: design and mechanism of action. Acc Chem Res 42:851–862
11. Caravan P, Cloutier NJ, Greenfield MT et al (2002) The interaction of MS-325 with human serum albumin and its effect on proton relaxation rates. J Am Chem Soc 124:3152–3162
12. Vander Elst L, Chapelle F, Laurent S et al (2001) Stereospecific binding of MRI contrast agents to human serum albumin: the case of Gd-(S)-EOB-DTPA (Eovist) and its ® isomer. J Biol Inorg Chem 6:196–200
13. Shen Y, Goerner FL, Snyder C et al (2015) T1 Relaxivities of Gadolinium-Based Magnetic Resonance Contrast Agents in Human Whole Blood at 1.5, 3, and 7 T. Investig Radiol 50:330–338
14. Morcos SK (2008) Extracellular gadolinium contrast agents: Differences in stability. Eur J Radiol 66:175–179
15. Laurent S, Vander Elst L, Henoumon C et al (2010) How to measure the transmetallation of a gadolinium complex. Contrast Media Mol Imaging 5:305–308
16. Laurent S, Vander Elst L, Copoix F et al (2001) Stability of MRI paramagnetic contrast media: a proton relaxometric protocol for transmetallation assessment. Investig Radiol 36:115–122
17. Aime S, Caravan P (2009) Biodistribution of gadolinium-based contrast agents, including gadolinium deposition. J Magn Res Imaging 30:1259–1267
18. Jung G, Heindel W, Krahe T et al (1998) Influence of the hepatobiliary contrast agent mangafodipir trisodium (MN-DPDP) on the imaging properties of abdominal organs. Magn Reson Imaging 16:925–931
19. Nelson SJ, Kurhanewicz J, Vigneron DB et al (2013) Metabolic imaging of patients with prostate cancer using hyperpolarized [1-^{13}C]pyruvate. Sci Transl Med 5:198ra108
20. Sieber MA, Steger-Hartmann T, Lengsfeld P et al (2009) Gadolinium-based contrast agents and NSF: evidence from animal experience. J Magn Res Imaging 30:1268–1276
21. Jost G, Lenhard DC, Sieber MA et al (2016) Signal increase on unenhanced T1-weighted images in the rat brain after repeated, extended doses of gadolinium-based contrast agents comparison of linear and macrocyclic agents. Investig Radiol 51:83–89
22. Anderson P (2015) FDA okays MRI contrast agent (Gadavist) in infants. Medscape. http://www.medscape.com/viewarticle/837629. Accessed 15 December 2016
23. Ellis JH, Davenport MS, Dillman JR et al (2015) ACR manual on contrast media v10.1. American College of Radiology, Reston
24. Grobner T (2006) Gadolinium — a specific trigger for the development of nephrogenic fibrosing dermopathy and nephrogenic systemic fibrosis? Nephrol Dial Transplant 21:1104–1108
25. Marckmann P, Skov L, Rossen K et al (2006) Nephrogenic systemic fibrosis: suspected causative role of gadodiamide used for contrast-enhanced magnetic resonance imaging. J Am Soc Nephrol 17:2359–2362
26. U.S. Food & Drug Administration (2009) Joint meeting of the Cardiovascular and Renal Drugs and Drug Safety and Risk Management Advisory Committee. Gadolinium-based contrast agents and nephrogenic systemic fibrosis: FDA briefing document. http://www.fda.gov/downloads/AdvisoryCommittees/CommitteesMeetingMaterials/Drugs/DrugSafetyandRiskManagementAdvisoryCommittee/UCM190850.pdf. Accessed 15 December 2016
27. Yang L, Krefting I, Gorovets A et al (2012) Nephrogenic systemic fibrosis and class labeling of gadolinium-based contrast agents by the Food and Drug Administration. Radiology 265:248–253
28. Swan SK, Lambrecht LJ, Townsend R et al (1999) Safety and pharmacokinetic profile of gadobenate dimeglumine in subjects with renal impairment. Investig Radiol 34:443–448
29. Marcos SK, Thomsen HS, Dawson P (2006) Is there a causal relation between the administration of gadolinium based contrast media and the development of nephrogenic systemic fibrosis (NSF)? Clin Radiol 61:905–906
30. Swan SK, Baker JF, Free R et al (1999) Pharmacokinetics, safety, and tolerability of gadoversetamide injection (OptiMARK) in subjects with central nervous system or liver pathology and varying degrees of renal function. J Magn Res Imaging 9:317–321
31. Schuhmann-Giampieri G, Krestin G (1991) Pharmacokinetics of Gd-DTPA in patients with chronic renal failure. Investig Radiol 26:975–979
32. European Medicines Agency (2010) Assessment report for gadolinium-containing contrast agents. Procedure no. EMEA/H/A-31/1097. http://www.ema.europa.eu/docs/en_GB/document_library/Referrals_document/gadolinium_31/WC500099538.pdf. Accessed 15 December 2016

33. Davenport MS, Dillman JR, Cohan RH et al (2013) Effect of abrupt substitution of gadobenate dimeglumine for gadopentetate dimeglumine on rate of allergic-like reactions. Radiology 266: 773–782
34. Hahn G, Sorge I, Gruhn B et al (2009) Pharmacokinetics and safety of gadobutrol-enhanced magnetic resonance imaging in pediatric patients. Investig Radiol 44:776–783
35. Kunze CW, Mentel H-J, Krishnamurthy R et al (2016) Pharmacokinetics and safety of macrocyclic gadobutrol in children aged younger than 2 years including term newborns in comparison to older populations. Investig Radiol 51:50–57
36. Kanda T, Kawaguchi H (2013) Hyperintense dentate nucleas and globus pallidus on unenhanced T1-weighted MR images are associated with gadolinium-based contrast media. Neuroradiology 55: 1268–1269
37. Kanda T, Ishii K, Kawaguchi H et al (2014) High signal intensity in the dentate nucleus and globus pallidus on unenhanced T1-weighted MR images: relationship with increasing cumulative dose of a gadolinium-based contrast material. Radiology 270: 834–841
38. Kanda T, Fukusato T, Matsuda M et al (2015) Gadolinium-based contrast agent accumulates in the brain even in subjects without severe renal dysfunction: evaluation of autopsy brain specimens with inductively coupled plasma mass spectroscopy. Radiology 276:228–232
39. Kanda T, Osawa M, Oba H et al (2015) High signal intensity in dentate nucleus on unenhanced T1-weighted MR images: association with linear versus macrocyclic gadolinium chelate administration. Radiology 275:803–809
40. Radbruch A, Weberling LD, Kieslich PJ et al (2015) Gadolinium retention in the dentate nucleus and globus pallidus is dependent on the class of contrast agent. Radiology 275:783–791
41. Miller JH, Houchun HH, Pokorney A et al (2015) MRI brain signal intensity changes of a child during the course of 35 gadolinium contrast examinations. Pediatrics 136:e1637–e1640
42. Murata N, Gonzalez-Cuyar LF, Murata K et al (2016) Macrocyclic and other non–group 1 gadolinium contrast agents deposit low levels of gadolinium in brain and bone tissue: preliminary results from 9 patients with normal renal function. Investig Radiol 51:447–453
43. Maximova N, Gregori M, Zennaro F et al (2016) Hepatic gadolinium deposition and reversibility after contrast agent-enhanced MR imaging of pediatric hematopoietic stem cell transplant recipients. Radiology 281:418–426
44. Chavhan GB, Babyn PS, John P et al (2015) Pediatric body MR angiography: principles, techniques, and current status in body imaging. AJR Am J Roentgenol 205:173–184
45. Grist TM, Thornton FJ (2005) Magnetic resonance angiography in children: technique, indications, and imaging findings. Pediatr Radiol 35:26–39
46. Miyazaki M, Akahane M (2012) Non-contrast enhanced MR angiography: established techniques. J Magn Reson Imaging 35:1–19
47. Chung T (2005) Magnetic resonance angiography of the body in pediatric patients: experience with a contrast-enhanced time-resolved technique. Pediatr Radiol 35:3–10
48. Rofsky NM, Lee VS, Laub G et al (1999) Abdominal MR imaging with a volumetric interpolated breath-hold examination. Radiology 212:876–884
49. Cornfield D, Mojibian H (2009) Clinical uses of time-resolved imaging in the body and peripheral vascular system. AJR Am J Roentgenol 193:W546–W557
50. Lewis M, Yanny S, Malcolm PN (2012) Advantages of blood pool contrast agents in MR angiography: a pictorial review. J Med Imaging Radiat Oncol 56:187–191
51. Krishnamurthy R, Bahouth SM, Muthapillai R (2016) 4D contrast-enhanced MR angiography with the keyhole technique in children: technique and clinical applications. Radiographics 36:14
52. Sundareswaran K, Frakes D, d Zelicourt D et al (2008) Comparison of power losses, hepatic flow splits, and vortex sizes in different fontan types using non invasive phase contrast magnetic resonance imaging. Circulation 118:S1057
53. Makowski M, Wiethoff A, Uribe S et al (2011) Congenital heart disease: cardiovascular MR imaging by using an intravascular blood pool contrast agent. Radiology 260:680–688
54. Hsiao A, Lustig M, Alley M et al (2012) Rapid pediatric cardiac assessment of flow and ventricular volume with compressed sensing parallel imaging volumetric cine phase-contrast MRI. AJR Am J Roentgenol 198:W250–W259
55. Gabbour M, Schnell S, Jarvis K et al (2015) 4-D flow magnetic resonance imaging: blood flow quantification compared to 2-D phase-contrast magnetic resonance imaging and Doppler echocardiography. Pediatr Radiol 45:804–813
56. Ordovas K, Higgins C (2011) Delayed contrast enhancement on MR images of myocardium: past, present, future. Radiology 261: 358–374
57. Simonetti O, Kim R, Fieno D et al (2001) An improved MR imaging technique for the visualization of myocardial infarction. Radiology 218:215–223
58. Kellman P, Wilson J, Xue H et al (2012) Extracellular volume fraction mapping in the myocardium, part 1: evaluation of an automated method. J Cardiovasc Magn Reson 14:63
59. Tandon A, Villa CR, Hor KN et al (2015) Myocardial fibrosis burden predicts left ventricular ejection fraction and is associated with age and steroid treatment duration in Duchenne muscular dystrophy. J Am Heart Assoc 4:e001338
60. O'Hanlon R, Grasso A, Roughton M et al (2010) Prognostic significance of myocardial fibrosis in hypertrophic cardiomyopathy. J Am Coll Cardiol 56:867–874
61. Moon J, Messroghli D, Kellman P et al (2013) Myocardial T1 mapping and extracellular volume quantification: a Society for Cardiovascular Magnetic Resonance (SCMR) and CMR Working Group of the European Society of Cardiology consensus statement. J Cardiovasc Magn Reson 15:92
62. Gerber B, Raman S, Nayak K et al (2008) Myocardial first-pass perfusion cardiovascular magnetic resonance: history, theory, and current state of the art. J Cardiovasc Magn Reson 10:18
63. Manso B, Castellote A, Dos L et al (2010) Myocardial perfusion magnetic resonance imaging for detecting coronary function anomalies in asymptomatic paediatric patients with a previous arterial switch operation for the transposition of great arteries. Cardiol Young 20:410–417
64. Prakash A, Powell A, Krishnamurthy R et al (2004) Magnetic resonance imaging evaluation of myocardial perfusion and viability in congenital and acquired pediatric heart disease. Am J Cardiol 93:657–661
65. Friedrich M, Sechtem U, Schulz-Menger J et al (2009) Cardiovascular magnetic resonance in myocarditis: a JACC white paper. J Am Coll Cardiol 53:1475–1487
66. Banka P, Robinson J, Uppu S et al (2015) Cardiovascular magnetic resonance techniques and findings in children with myocarditis: a multicenter retrospective study. J Cardiovasc Magn Reson 17:96
67. Ferreira V, Piechnik S, Dall'Armellina E et al (2012) T1-mapping has a high diagnostic performance in patients presenting with acute myocarditis: a cardiovascular magnetic resonance study. Heart 98:A52–A53
68. Ferreira V, Piechnik S, Dall'Armellina E et al (2013) T(1) mapping for the diagnosis of acute myocarditis using CMR: comparison to T2-weighted and late gadolinium enhanced imaging. JACC Cardiovasc Imaging 6:1048–1058
69. Seale MK, Catalano OA, Saini S et al (2009) Hepatobiliary-specific MR contrast agents: role in imaging the liver and biliary tree. Radiographics 29:1725–1748

70. Tran VT, Vasanawala S (2013) Pediatric hepatobiliary magnetic resonance imaging. Radiol Clin N Am 51:599–614
71. Guglielmo FF, Mitchell DG, Gupta S (2014) Gadolinium contrast agent selection and optimal use for body MR imaging. Radiol Clin N Am 52:637–656
72. Nandwana SB, Moreno CC, Osipow MT et al (2015) Gadobenate dimeglumine administration and nephrogenic systemic fibrosis: is there a real risk in patients with impaired renal function? Radiology 276:741–747
73. Lauenstein T, Ramirez-Garrido F, Kim YH et al (2015) Nephrogenic systemic fibrosis risk after liver magnetic resonance imaging with gadoxetate disodium in patients with moderate to severe renal impairment: results of a prospective, open-label, multicenter study. Investig Radiol 50:416–422
74. Vaneckova M, Herman M, Smith MP et al (2015) The benefits of high relaxivity for brain tumor imaging: results of a multicenter intraindividual crossover comparison of gadobenate dimeglumine with gadoterate meglumine (The BENEFIT study). AJNR Am J Neuroradiol 36:1589–1598
75. Rigsby CK, Popescu AR, Nelson P et al (2015) Safety of blood pool contrast agent administration in children and young adults. AJR Am J Roentgenol 205:1114–1120
76. Rigsby CK, Hilpipre N, McNeal GR et al (2014) Analysis of an automated background correction method for cardiovascular MR phase contrast imaging in children and young adults. Pediatr Radiol 44:265–273
77. Farmakis SG, Khanna G (2014) Extracardiac applications of MR blood pool contrast agent in children. Pediatr Radiol 44: 1598–1609
78. Cha S (2006) Dynamic susceptibility-weighted contrast-enhanced perfusion MR imaging in pediatric patients. Neuroimaging Clin N Am 16:137–147
79. Wang Y-XJ, Hussain SM, KRestin GP (2001) Superparamaganetic iron oxide contrast agents: physicochemical characteristics and applications in MR imaging. Eur Radiol 11:2319–2331
80. Wang Y-XJ (2011) Superparamagnetic iron oxide based MRI contrast agents: current status of clinical application. Quant Imaging Med Surg 11:35–40
81. Hope MD, Hope TA, Zhu C et al (2015) Vascular imaging with ferumoxytol as a contrast agent. AJR Am J Roentgenol 205: W366–W374
82. Bellin M-F, Roy C, Kinkel K et al (1998) Lymph node metastases: safety and effectiveness of MR imaging with ultrasmall superparamagnetic iron oxide particles —initial clinical experience. Radiology 207:799–808
83. Li S-D, Huang L (2008) Pharmacokinetics and biodistribution of nanoparticles. Mol Pharm 5:496–504
84. Arami H, Khandhar A, Liggitt D et al (2015) In vivo delivery, pharmacokinetics, biodistribution and toxicity of iron oxide nanoparticles. Chem Sci Rev 44:8576–8607
85. Li W, Tutton S, Vu AT et al (2004) First-pass contrast-enhanced magnetic resonance angiography in humans using ferumoxytol, a novel ultrasmall superparamagnetic iron oxide (USPIO)-based blood pool agent. J Magn Res Imaging 21:46–52
86. Harisinghani MG, Berentsz J, Hahn PF et al (2003) Noninvasive detection of clinically occult lymph-node metastases in prostate cancer. N Engl J Med 348:2491–2499
87. Heesakkers RAM, Jager GJ, Hövels AM et al (2009) Prostate cancer: detection of lymph node metastases outside the routine surgical area with ferumoxtran-10 - enhanced MR imaging. Radiology 251:408–414
88. Prince MR, Zhang HL, Chabra SG et al (2003) A pilot investigation of new superparamagnetic iron oxide (ferumoxytol) as a contrast agent for cardiovascular MRI. J Xray Sci Technol 11:231–240
89. Ruangwattanapaisarn N, Hsiao A, Vasanawala SS (2015) Ferumoxytol as an off-label contrast agent in body 3T MR angiography: a pilot study in children. Pediatr Radiol 45:831–839
90. Luhar A, Khan S, Finn JP et al (2016) Contrast-enhanced magnetic resonance venography in pediatric patients with chronic kidney disease: initial experience with ferumoxytol. Pediatr Radiol 46:1332–1340
91. Thompson EM, Guillaume DJ, Dósa E et al (2012) Dual contrast perfusion MRI in a single imaging session for assessment of pediatric brain tumors. J Neurooncol 109:105–114
92. Schiller B, Bhat P, Sharma A (2014) Safety and effectiveness of ferumoxytol in hemodialysis patients at 3 dialysis chains in the United States over a 12-month period. Clin Ther 36:70–83
93. Muehe AM, Fang D, von Eyben R et al (2016) Safety report of ferumoxytol for magnetic resonance imaging in children and young adults. Investig Radiol 51:221–227
94. Lauffer RB (1987) Paramagnetic metal complexes as water proton relaxation agents for NMR imaging: theory and design. Chem Rev 87:901–927
95. Elizondo G, Fretz CJ, Stark DD et al (1991) Preclinical evaluation of MnDPDP: new paramagnetic hepatobiliary contrast agent for MR imaging. Radiology 178:73–78
96. Hamm B, Vogl TJ, Branding G et al (1992) Focal liver lesions: MR imaging with MnDPDP initial clinical results in 40 patients. Radiology 182:167–174
97. Vogl TJ, Hamm B, Schnell B et al (1993) Mn-DPDP enhancement patterns of hepatocellular lesions on MR images. J Magn Res Imaging 3:51–58
98. Gallez B, Bacic G, Swartz HM (1996) Evidence for the dissociation of the hepatobiliary MRI contrast agent Mn-DPDP. Magn Reson Med 35:14–19
99. Toft KG, Hustvedt SO, Grat D et al (1997) Metabolism and Pharmacokinetics of MnDPDP in man. Acta Radiol 38:677–689
100. Crossgrove J, Zheng W (2004) Manganese toxicity upon overexposure. NMR Biomed 17:544–553
101. O'Neal SL, Zheng W (2015) Manganese toxicity upon overexposure: a decade in review. Curr Environ Health Rep 2:315–328
102. Aschner JL, Aschner M (2005) Nutritional aspects of manganese homeostasis. Mol Asp Med 26:353–362
103. Yang Y, Schühle DT, Dai G et al (2012) 1H chemical shift magnetic resonance imaging probes with high sensitivity for multiplex imaging. Contrast Media Mol Imaging 7:276–279
104. Harvey P, Blamire AM, Wilson JI et al (2013) Moving the goal posts: enhancing the sensitivity of PARASHIFT proton magnetic resonance imaging and spectroscopy. Chem Sci 4:4251–4258
105. Mizukami S, Takikawa R, Sugihara F et al (2008) Paramagnetic relaxation-based 19F MRI probe to detect protease activity. J Am Chem Soc 130:794–795
106. Tirotta I, Mastropietro A, Cordiglieri C et al (2014) A superfluorinated molecular probe for highly sensitive in vivo19F-MRI. J Am Chem Soc 136:8524–8527
107. Sherry AD, Woods M (2008) Chemical exchange saturation transfer contrast agents for magnetic resonance imaging. Annu Rev Biomed Eng 10:391–411
108. Liu G, Gilad AA, Bulte JWM et al (2010) High-Throuput Screening of Chemical Exchange Saturation Transfer MR Contrast Agents. Contrast Media Mol Imaging 5:162–170
109. Brindle KM, Bohndiek SE, Gallagher FA, Kettunen MI (2011) Tumor imaging using hyperpolarized 13C magnetic resonance spectroscopy. Magn Reson Med 66(2):505–19
110. Svenningsen S, Kirby M, Starr D et al (2013) Hyperpolarized 3He and 129Xe MRI: differences in asthma before bronchodilation. J Magn Res Imaging 38:1521–1530
111. Qing K, Ruppert K, Jiang Y et al (2014) Regional mapping of gas uptake by blood and tissue in the human lung using hyperpolarized xenon-129 MRI. J Magn Reson Imaging 39:346–359